IX. Cosmic Microwave Background (CMB) Anistropies

Excellent sources of information on CMB anisotropy are Wayne Hu's web site

`http://background.uchicago.edu`

for discussions of the physics of the anisotropies and Max Tegmark's web site

`http://space.mit.edu/home/tegmark`

(follow the CMB experiments and CMB movies links) for discussions of experimental results and cosmological parameter constraints.

For reading, I suggest *Cosmic Microwave Background Anisotropies*, Hu & Dodelson 2002, Annual Reviews of Astronomy and Astrophysics; you can get a copy from Hu's web page. Reading it is a substantial amount of work, but it covers all of the theoretical ground very well.

Kosowsky et al. (2002, Phys Rev D, 66, 063007) offer considerable insight into the information content of the CMB and ways of thinking about the cosmological constraints that can be derived from it.

Tegmark et al. (2006, Phys Rev D, 74, 123507) is one of the best discussions on joint cosmological constraints from CMB anisotropy and galaxy large scale structure, from WMAP and the SDSS, respectively. It is particularly good on the dependence of the constraints on assumed model space and priors.

Physical Sources of Anisotropy

If the universe is inhomogeneous at last scattering, then the CMB should be anisotropic.

There are many effects that produce anisotropy.

Primary anisotropies arise at recombination and during the subsequent free-streaming of photons:

- temperature variations present at recombination – higher photon energy density $\Longrightarrow$ higher T
- gravitational redshift of photons
- time-variable gravitational potential
- Doppler shifts from fluid motion at last scattering
- gravitational waves (a.k.a. tensor fluctuations)

The combination of the first 3 on large angular scales is known as the "Sachs-Wolfe effect," sometimes divided into "Sachs-Wolfe" (first two) and "integrated Sachs-Wolfe" (third) because the third comes from non-trivial contributions to the integral along the photon path.

Secondary anisotropies arise when photons are re-scattered at low redshift:

- Doppler shifts at secondary scattering
- Thermal Sunyaev-Zel'dovich effect (scattering by hot gas in clusters)

Because CMB photons scatter off of moving electrons, the CMB fluctuations are expected to be polarized (at roughly the 10% level).

Gravitational lensing has a weak but potentially detectable effect on anisotropies.

Observationally, CMB anisotropies must be distinguished from foreground "contamination," such as:

- Discrete radio sources
- Thermal emission by Galactic dust
- Radiation from spinning dust grains
- Galactic synchrotron emission

These can be distinguished from the intrinsic anisotropy because they do not have a blackbody spectrum. The last three also have a different sky distribution, and discrete radio sources contribute only on small angular scales.

Characterization of CMB Anisotropies

Suppose we have a map of the CMB temperature fluctuations $\Delta T(\theta, \phi)/T$ over the whole sky (where T in the numerator is the mean temperature).

Just as it is convenient to work with Fourier modes of 3-d fluctuations, it is convenient to decompose the CMB into spherical harmonics Y_{lm}:

$$\frac{\Delta T(\theta, \phi)}{T} = \sum_{l,m} a_{lm} Y_{lm}(\theta, \phi).$$

By definition $\langle a_{lm} \rangle = 0$. The mean squared expectation value of a_{lm} is called the angular power spectrum,

$$C_l \equiv \langle |a_{lm}^2| \rangle.$$

The typical temperature fluctuation for a CMB map smoothed over an angle θ is dominated by multipoles $l \approx 100^\circ/\theta$, with variance

$$\left\langle \left(\frac{\Delta T}{T} \right)^2 \right\rangle_\theta \approx l(l+1) C_l / 2\pi |_{l \approx 100^\circ/\theta}.$$

CMB Power Spectrum Measurements: First Look

As shown in these data compilations by Max Tegmark (see second-to-last page), the fluctuation spectrum $l(l+1)C_l$:

- is flat from $l \sim 3 - 30$
- rises to a clear peak at $l \sim 220$
- shows clear evidence of a second, lower amplitude peak and a reasonable hint of a third peak
- tails off slowly towards higher l
- has a low quadrupole ($l = 2$) relative to the low-l plateau, though the error bar is big

Most of these features are well explained by an inflationary cold dark matter model with appropriate choice of the free parameters (which are numerous, but far fewer than the number of data points).

Adiabatic and Isocurvature Initial Conditions

On scales much larger than the Hubble radius cH^{-1}, there has not been time to transport energy from one region to another.

The "initial conditions" when a fluctuation is larger than the Hubble radius can be

- *Adiabatic* perturbations (a.k.a. curvature perturbations, energy perturbations): The total energy is perturbed, hence so is the spacetime curvature. Positive matter fluctuation $\Longrightarrow$ positive radiation fluctuation.
- *Isocurvature* (a.k.a. entropy): The matter-radiation mix is perturbed, but there is no perturbation to the total energy and hence no curvature perturbation on scales larger than cH^{-1}. Positive matter fluctuation $\Longrightarrow$ negative radiation fluctuation.

Inflation generically produces adiabatic fluctuations.

Other causal mechanisms can only produce isocurvature fluctuations, since they cannot transport energy on scales larger than the horizon.

After a scale enters the Hubble radius, pressure gradients can move material over the scale of the perturbation, so isocurvature perturbations eventually evolve into energy and curvature perturbations.

There are various flavors of isocurvature fluctuations, since radiation, baryons, CDM, and neutrinos can be perturbed differently, and some mechanisms generate the fluctuations at horizon crossing rather than imprinting them in the early universe.

The Close Coupling Approximation

A good approximation for CMB calculations is to treat the photons and baryons as a single, ideal fluid prior to recombination, since Thomson scattering makes it very difficult for photons to diffuse relative to baryons.

This approximation has been used to particularly good effect by Wayne Hu and Naoshi Sugiyama, who have demonstrated its usefulness by comparing to fully numerical solutions.

This fluid has a high sound speed $c_s = c/\sqrt{3(1+R)}$, with $R \equiv 3\rho_b/4\rho_\gamma$, and it evolves in the potential wells provided by the (uncoupled) cold dark matter.

One can derive equations for the spatial Fourier modes as a function of conformal time $\eta \equiv \int (1+z)dt$.

Photons decouple from baryons at last scattering $\eta = \eta_*$ (i.e., $t = t_*$, where $*$ denotes recombination), and we see a "snapshot" of the temperature distribution at that time.

A Fourier mode describes a pattern of $+/-$ fluctuations varying on a scale $\lambda \sim 2\pi/k$.

Since negative fluctuations do just the opposite of positive fluctuations in linear theory, we can get intuition for the evolution of Fourier modes by thinking about the evolution of a single, overdense, quasi-spherical perturbation of scale π/k.

The Sachs-Wolfe Effect and Acoustic Oscillations

An overdense perturbation will begin to collapse under its own gravity.

If there is sufficient time a pressure gradient can build up to halt the collapse and cause the perturbation to re-expand and overshoot the mean density.

The time for a sound wave to cross a perturbation is $t_{\rm cross} \sim (kc_s/\pi)^{-1}$, so this divides two critical regimes:

$t_{\rm cross} \gg t_*$: no time for pressure to act before recombination.

Fluctuations come from intrinsic temperature and gravitational redshift.

Adiabatic initial conditions: These two effects are opposite in sign — photons in overdense regions must climb out of CDM potential wells.

Gravitational redshift effect wins, overdense regions are (slightly) colder, $\Delta T/T \sim \Phi/3$ where $\Phi \sim -G\delta M/Rc^2$ is the gravitational potential fluctuation associated with a mass fluctuation $\delta M = (4\pi/3)R^3\bar{\rho}(\delta\rho/\bar{\rho})$ of physical (not comoving) radius R.

Isocurvature initial conditions: The two effects add — regions that are overdense in CDM have colder photons, *and* these must climb out of the potential wells.

Overdense regions are (much) colder, $\Delta T/T \sim 2\Phi$.

$t_{\rm cross} \lesssim t_*$: photon pressure causes perturbations to oscillate in time, so temperature fluctuation oscillates from positive to negative and back.

Decoupling catches oscillations at different phases, hence different amplitudes depending on scale.

Oscillation of fluctuations in time with different frequencies leads to oscillation of typical $\Delta T/T$ amplitude with physical scale.

Contraction/expansion produces Doppler shifts, which are 90° out of phase with compression/rarefaction.

Therefore, the troughs between peaks don't fall to zero, but they are troughs because the Doppler shift effect is weaker than the actual energy density fluctuations.

The Integrated Sachs-Wolfe Effect

After recombination, photons free-stream, but they are still affected by gravitational redshifts and blueshifts.

If $\Omega = \Omega_m = 1$, $\Phi \sim G\delta M/R$ is independent of time because $\delta M \propto a(t)$ and $R \propto a(t)$.

If a photon falls into a potential well along the way to the observer, it must climb out of the same potential well, so there is no net redshift or blueshift.

But if radiation, curvature, or vacuum energy are important, then δM grows slower than $a(t)$, and the photon climbs out of a shallower potential well than it fell into.

The contribution to anisotropy from redshifts/blueshifts in time-varying gravitational potential wells is called the integrated Sachs-Wolfe (ISW) effect.

The "early" ISW effect occurs near recombination, where radiation is a significant contribution to the energy density, and it affects relatively small angular scales (a few times $ct_{\rm eq}/D_*$, where D_* is the angular diameter distance to redshift z_*).

The "late" ISW effect occurs at low redshift, if curvature or vacuum energy modify $a(t)$. It affects large angular scales, comparable to the present horizon; on smaller scales, a photon goes through many $+/-$ fluctuations while the potential decays.

Non-linear gravitational evolution also breaks $\delta M \propto a(t)$; this non-linear contribution to the ISW anisotropy is often called the "Rees-Sciama effect."

Damping on small scales

The last scattering surface has a finite width, $\Delta z \approx 80$.

Anisotropies are damped on scales smaller than this, since photons from positive and negative fluctuations are mixed together.

For standard recombination, the damping scale is small, a few arc-minutes

For early reionization, implying late last scattering, the damping scale is much larger.

Late scattering produces a polarization signal at large angles. Polarization measurements from the 3-year WMAP data imply an optical depth $\tau \approx 0.1$.

For instantaneous reionization, this optical depth implies a hydrogen reionization redshift $z_r \approx 11$.

This low redshift scattering suppresses the amplitude of the power spectrum by $e^{-2\tau}$, except at large ($>$ several degree) angles.

Projection

A given physical scale translates to an angular scale at the last scattering surface, $\theta \sim \lambda/D_*$, where D_* is the angular diameter distance at z_*.

Fourier modes have different orientations, so characteristic scales (e.g., of acoustic oscillations) are broader in angular space than in physical space.

The main effect in translating physical to angular scales is space geometry. In an open universe, features appear at smaller angular scale and thus higher l.

In a flat universe, D_* scales roughly as $\Omega_m^{1/2}$, so higher Ω_Λ decreases angular scales for fixed physical scales.

However, the physical scale of the acoustic peaks is also approximately $\propto \Omega_m^{1/2}$, so the angular scale of the peaks is only weakly sensitive to Ω_m for a flat universe.

CMB Anisotropy: Main Points

Constraining power

Different physical effects dominate on different scales.

The relative amplitude of these effects, and the angular scales at which they appear, depend on the initial conditions and on cosmological parameters (Ω_m, Ω_b, Ω_Λ, etc.).

Tegmark's CMB movies page nicely illustrates the dependence on parameters.

Precise measurements over a wide range of scales therefore have power to break degeneracy between initial conditions and cosmological parameters and among parameters themselves.

Initial conditions

At large angles, a scale-invariant inflationary spectrum (δ_H =const.) corresponds approximately to a flat CMB power spectrum $l(l+1)C_l$.

This is roughly what is observed, though the quadrupole ($l = 2$) is surprisingly low.

A tilt (departure from constant δ_H, or equivalently from $n = 1$) in the inflationary fluctuation spectrum adds an overall tilt to the CMB power spectrum.

Adiabatic initial conditions lead to coherent oscillations and hence to a series of well defined acoustic peaks.

Isocurvature initial conditions do not produce such a clear series of peaks, and the peaks they do produce tend to have different shapes and locations.

The first two peaks are clearly well defined, with the shape and l-ratio of $2:1$ expected for adiabatic initial conditions, indicating that fluctuations were (at least mainly) adiabatic, as inflation predicts.

Acoustic peaks

The scales and amplitudes of the peaks depend mainly on physical densities $\Omega_m h^2$ and $\Omega_b h^2$ rather than Ω_m and Ω_b directly.

The *physical* scale of the first acoustic peak is set by the sound horizon at recombination, roughly $c_s t_*$, where $c_s = c/\sqrt{3(1+R)}$ is the sound speed of the photon-baryon fluid, with the baryon/photon density ratio $R = \rho_b/(4\rho_\gamma/3) \sim 1$ at t_* for typical $\Omega_b h^2$.

The *angular* scale of the first acoustic peak is set by $c_s t_*/D_*$, where D_* is the angular diameter distance to the surface of last scattering.

This combination is thus extremely well determined by CMB data.

An open ($k = -1$) geometry shifts all acoustic peaks to smaller angular scales because it increases D_*.

The location of the first peak at $l \sim 220$ rules out a universe with $\Omega_k \sim 0.7$, since a strongly open geometry would increase D_* and shift the peak to higher l.

The location agrees well with the prediction for a flat universe for plausible values of other parameters.

The peak location is only mildly sensitive to Ω_Λ in a flat universe because t_* and D_* both scale in a similar way with Ω_m.

Decreasing $\Omega_m h^2$ increases the amplitude of the acoustic peaks.

Increasing $\Omega_b h^2$ increases the amplitude of the *odd* peaks (first, third, fifth) and suppresses the amplitude of the even peaks, because the baryon self-gravity enhances compressional peaks relative to rarefaction peaks.

The relative amplitudes of the acoustic peaks are therefore good diagnostics for $\Omega_m h^2$ and $\Omega_b h^2$.

Secondary scattering

On small angular scales, anisotropies are suppressed by mixing over the finite width of the last scattering surface.

Anisotropies at $l \gtrsim 3000$ are likely to be dominated by secondary effects.

Low-redshift scattering suppresses C_l by $e^{-2\tau}$ except at the largest scales, so there are tradeoffs between reionization, the overall amplitude of fluctuations, and tilt of the inflationary spectrum.

Large-angle polarization is an independent way of estimating τ.

Gravity waves

Gravity waves could also be contributing to large angle anisotropies, though they redshift after entering the horizon and are therefore unimportant at small scales.

A clear detection of the gravity wave contribution would be a valuable test/diagnostic of inflationary models, since the spectrum of gravity waves depends on the energy scale and form of the inflationary potential.

Prospects

As a probe of cosmology, CMB anisotropies have the enormous virtue of being described well by linear perturbation theory, without complicated gas physics.

Current and, even more, future CMB observations (e.g., the Planck satellite at the end of the decade) will yield extremely precise constraints on several combinations of cosmological parameters.

However, there are also some strong parameter degeneracies, which must be broken using independent data at lower redshifts.

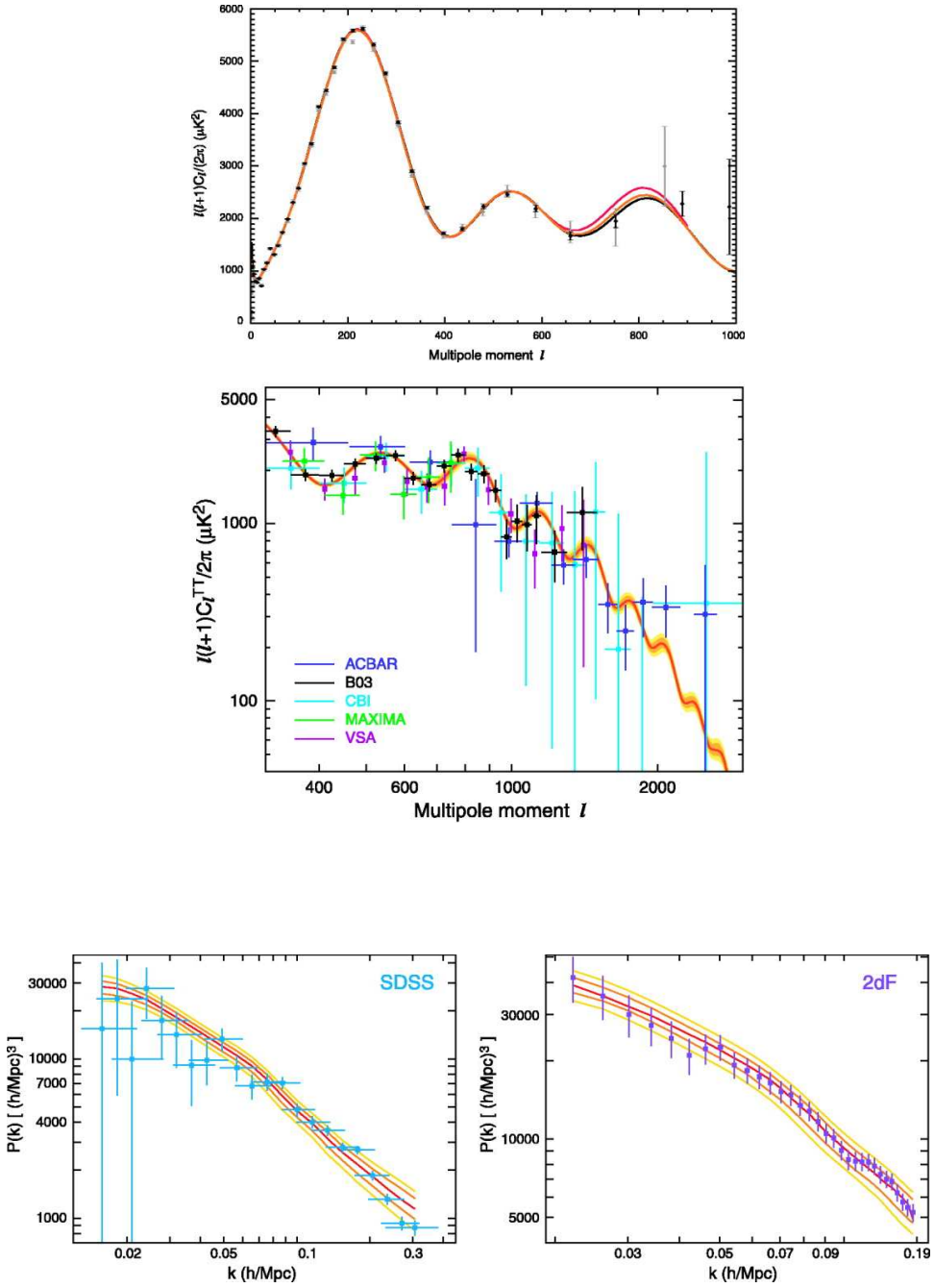

Figures from Spergel et al. 2007, ApJS 170, 377.

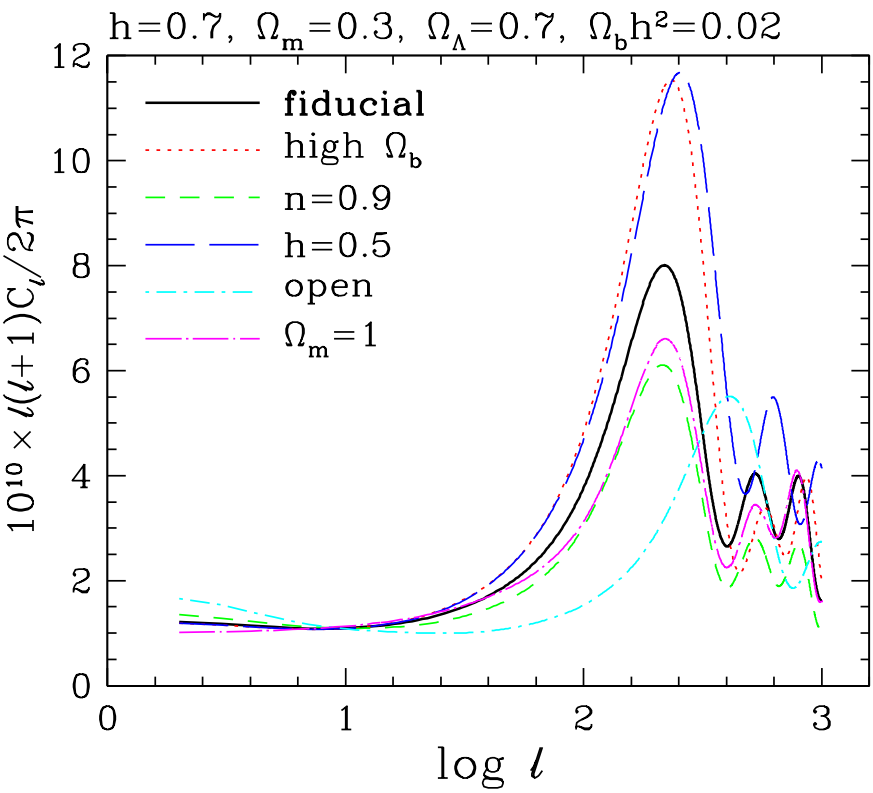
h=0.7, Ωm=0.3, ΩΛ=0.7, Ωbh²=0.02
fiducial
high Ωb
n=0.9
h=0.5
open
Ωm=1
10¹⁰ × l(l+1)Cl/2π
log l
0
1
2
3
0
2
4
6
8
10
12

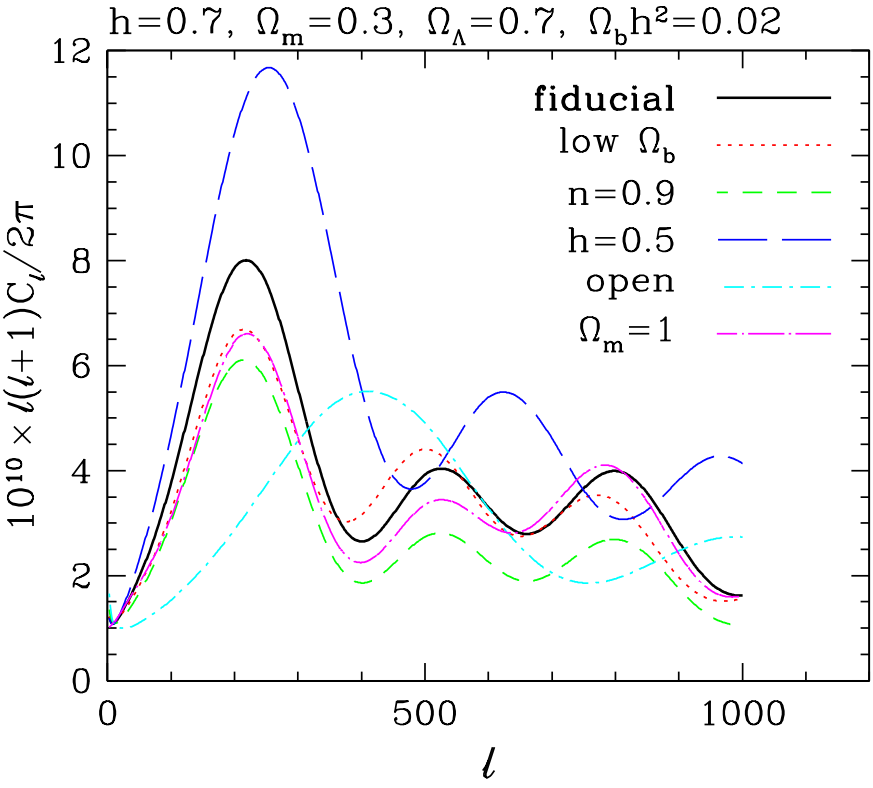
h=0.7, Ωm=0.3, ΩΛ=0.7, Ωbh²=0.02
fiducial
low Ωb
n=0.9
h=0.5
open
Ωm=1
10¹⁰ × l(l+1)Cl/2π
l
0
500
1000
0
2
4
6
8
10
12